Available online at www.sciencedirect.com

ScienceDirect

www.elsevier.com/locate/jes

JES JOURNAL OF ENVIRONMENTAL SCIENCES

www.jesc.ac.cn

Understanding the electrode reaction process of dechlorination of 2,4-dichlorophenol over Ni/Fe nanoparticles: Effect of pH and 2,4-dichlorophenol concentration

Kaiyuan Zheng[1,2], *Yuqiao Song*[1,2], *Xu Wang*[1,2,*], *Xin Li*[1,2], *Xuhui Mao*[1,2], *Dihua Wang*[1,2,*]

1. *School of Resources and Environmental Sciences, Wuhan University, Wuhan 430079, China*
2. *Hubei International Scientific and Technological Cooperation Base of Sustainable Resource and Energy, Wuhan University, Wuhan 430079, China*

ARTICLE INFO

Article history:
Received 8 June 2018
Revised 7 January 2019
Accepted 14 January 2019
Available online 23 January 2019

Keywords:
2,4-Dichlorophenol (2,4-DCP)
Dechlorination
Corrosion
Catalytic hydrogenation
Ni/Fe particles

ABSTRACT

Herein, with the exploitation of iron and nickel electrodes, the 2,4-dichlorophenol (2,4-DCP) dechlorinating processes at the anode and cathode, respectively, were separately studied via various electrochemical techniques (e.g., Tafel polarization, linear polarization, electrochemical impedance spectroscopy). With this in mind, Ni/Fe nanoparticles were prepared by chemical solution deposition, and utilized to test the dechlorination activities of 2,4-DCP over a bimetallic system. For the iron anode, the results showed that higher 2,4-DCP concentration and solution acidity aggravated the corrosion within the electrode. The charge transfer resistance (R_{ct}) values of the iron electrode were 703, 473, 444, and 437 $\Omega \cdot cm^2$ for the initial 2,4-DCP concentrations of 0, 20, 50, and 80 mg/L, respectively. When the bulk pH of the 2,4-DCP solution varied from 3.0, 5.0 to 7.0, the corresponding R_{ct} values were 315, 376, and 444 $\Omega \cdot cm^2$, respectively. For the nickel cathode, the reduction current densities on the electrode at −0.75 V (vs. saturated calomel electrode) were 80, 106, and 111 $\mu A/cm^2$, for initial 2,4-DCP concentrations of 40, 80, and 125 mg/L. The dechlorination experiments demonstrated that when the initial pH of the solution was 7.0, 5.0, and 3.0, the dechlorination percentage of 2,4-DCP by Ni/Fe nanoparticles was 62%, 69%, and 74%, respectively, which was in line with the electrochemical experiments. 10 wt.% Ni loading into Ni/Fe bimetal was affordable and gave a good dechlorination efficiency of 2,4-DCP, and fortunately the Ni/Fe nanoparticles remained comparatively stable in the dechlorination processes at pH 3.0.

Introduction

Chlorophenols (CPs) are widely found in wastewaters from pesticides, dyes, and the pharmaceutical and petroleum industries (Gupta et al., 2004; Pera-Titus et al., 2004). Most of them are persistent organic contaminants and their biological accumulation through the food chain poses a great threat to the health of humans and wildlife (Wang et al., 2013, 2015).

* *Corresponding authors. E-mails:* xu.wang@whu.edu.cn (Xu Wang), wangdh@whu.edu.cn (Dihua Wang).

https://doi.org/10.1016/j.jes.2019.01.012
1001-0742 © 2019 The Research Center for Eco-Environmental Sciences, Chinese Academy of Sciences. Published by Elsevier B.V.

Most chlorophenols are listed as priority pollutants (Liu et al., 2001).

Nano zero-valent iron (nZVI, Fe^0) forms redox couples with numerous electron acceptors in wastewater and holds great promise for aquatic environmental remediation because of its low cost, good reactivity, and environmental compatibility (Crane and Scott, 2012; Phenrat et al., 2007). In the past decades, Fe^0 nanoparticles have been shown to be effective in the dechlorination process of CPs (Liu et al., 2001; Su et al., 2011; Zhou et al., 2010). To further enhance the reactivity and functionality, a second metal (e.g., Ni or Pd) is often deposited onto the Fe^0 surface to synthesize iron-based bimetallic particles (Wang et al., 2014; Zahran et al., 2013; Zhang et al., 2015; Zhou et al., 2011).

From the perspective of physical chemistry, the dechlorination of CPs over the bimetallic system more likely takes place via a galvanic cell reaction (Su et al., 2011; Zhang et al., 2006). In Ni/Fe bimetallic system, Fe has a lower redox potential (E^0 = −0.44 V) and is able to donate electrons to Ni (a higher redox potential, E^0 = −0.25 V). The reaction activity of dechlorination is able to be enhanced because the corrosion of Fe can be accelerated by the potential difference. Meanwhile, as a typical hydrogenation catalyst, Ni in the bimetallic system is able to utilize hydrogen ions (i.e., protons) in wastewater and dissociate the H_2 produced from Fe. Therefore, Ni/Fe bimetallic particles have shown higher efficiencies for dechlorination than Fe alone. The anode reaction in the aforementioned galvanic cell is the sacrifice of iron, namely iron corrosion, providing electrons (Eq. (1)):

$$Fe^0 \rightarrow Fe^{2+} + 2e^- \quad (1)$$

Cathode reaction: H_2 and H^+ absorbed and dissociated on the second metal (Ni or Pd) form hydrogen radicals (H^*) and catalyze the dechlorination of chlorophenols. The reactions can be depicted as Eqs. (2)–(6) (Zhang et al., 2006; Wang and Wang, 2009).

$$2H^+ + 2e^- \rightarrow H_2 \quad (2)$$

$$2H_2O + 2e^- \rightarrow H_2 + 2OH^- \quad (3)$$

$$H_2 \xrightarrow{Ni} 2H^* \quad (4)$$

$$H^+ + e^- \xrightarrow{Ni} H^* \quad (5)$$

$$2H^* + R\text{-}Cl \rightarrow R\text{-}H + H^+ + Cl^- \quad (6)$$

Extensive studies have been conducted to improve the dechlorination performance by optimizing the bimetallic composition, temperature, and other experimental conditions (Chen et al., 2014; Jovanovic et al., 2015; Wei et al., 2014; Xu et al., 2013). Reaction pathways have been proposed according to the dechlorination efficiency of CPs and the formation of intermediates. However, no experimental study has been reported on the electrode process of dechlorination on a bimetallic system in such galvanic cells. The effects of chlorophenol concentration and pH on the electrode process of iron corrosion or hydrogenation catalysis for the Ni/Fe bimetallic system have not been clearly elucidated.

In this study, we chose the dechlorination of 2,4-dichlorophenol (2,4-DCP) over Ni/Fe bimetal as a typical galvanic cell system. An H-type electrolytic cell was set up to simulate the dechlorination by Ni/Fe nanoparticles. The anodic and cathodic electrode processes of dechlorination were investigated separately using an iron electrode and a nickel electrode by various electrochemical techniques. The effects of CP concentration and pH on the electrode kinetics were investigated. Furthermore, Ni/Fe bimetallic particles were prepared and the dechlorination performance of 2,4-DCP over Ni/Fe bimetallic particles was characterized. The objectives of this work are: (a) to study the electrode process of dechlorination over the Ni/Fe bimetallic system; (b) to provide an electrochemical explanation for the effect of pH and initial concentration on dechlorination.

1. Materials and methods

1.1. Chemicals

2,4-DCP (chemically pure (CP) grade), nickel chloride hexahydrate (analytical reagent (AR) grade), iron sulfate heptahydrate (AR grade), and sodium sulfate (AR grade) were obtained from Sinopharm Chemical Reagent, and nickel sulfate hexahydrate (CP grade) was obtained from Aladdin Reagent. Sodium borohydride (AR grade) was purchased from Tianjin Chemical Reagent.

1.2. Electrochemical experiments

1.2.1. Anodic process on iron electrode

The electrochemical measurements were conducted in a two-compartmentglass-jacketed cell (each compartment volume: 140 mL). The anodic and cathodic compartments were separated by a 9.0 cm^2 cation-exchange membrane (Nafion-117, DuPont, USA). A 1.0 cm^2 Fe sheet (Puratronic 99.99%) mounted in Teflon was used as the working electrode. A saturated calomel electrode (SCE) and a platinum foil of 4.0 cm^2 were used as reference and counter electrodes, respectively. All electrochemical experiments were conducted at 25°C. The anodic compartment contained 100 mL of a 0.1 mol/L Na_2SO_4 aqueous solution with various amounts of 2,4-DCP, and the cathodic compartment contained 100 mL of 0.1 mol/L Na_2SO_4 aqueous solution. Before the measurements, the whole system was stabilized for 15 min to attain a steady open circuit potential (E_{oc}).

Polarization resistances and polarization curves were measured by a CHI660D electrochemical workstation. Linear scan voltammetry (LSV) curves were analyzed from −10 to +10 mV versus E_{oc} with 0.5 mV/sec scan rate. Tafel polarization measurements were determined by changing the electrode potential from −200 to +200 mV (vs. E_{oc}) with 0.5 mV/sec scan rate. Electrochemical impedance spectroscopy (EIS) measurements were carried out from 100 kHz to 10 mHz. The amplitude was 5 mV. EIS measurements were performed with an electrochemical system (PAR M2273, Ametek, USA).

1.2.2. Cathodic process on nickel electrode

The measurements of the cathodic process were also performed in the H-cell with three-electrode system at

25°C. A 1.0 cm^2 nickel sheet (Puratronic, 99.99%) mounted in Teflon was used as the working electrode. A saturated calomel electrode and a platinum foil of 4.0 cm^2 were used as reference and counter electrodes, respectively. Linear scan voltammetry analysis for the cathodic process was performed by changing the electrode potential from −0.31 to −0.75 V (vs. E_{oc}) with 0.5 mV/sec scan rate and measured by the CHI660D instrument. The catholyte was 100 mL of 0.1 mol/L Na_2SO_4 aqueous solution containing a certain amount of 2,4-DCP. The anolyte was 100 mL of 0.1 mol/L Na_2SO_4 aqueous solution.

1.3. Synthesis and characterization of Ni/Fe nanoparticles

The Ni/Fe nanoparticles were prepared according to the procedures reported by Zhao et al. (2014) and Xu et al. (2009). The iron nanoparticles (ZVI) were prepared by dropwise addition of a stoichiometric amount of $NaBH_4$ aqueous solution into a 500 mL three-necked flask containing $FeSO_4{\cdot}7H_2O$ aqueous solution with stirring. The Fe^0 particles were precipitated and then washed several times with deionized water. Subsequently, Ni/Fe nanoparticles were prepared by reacting the freshly prepared nanoscale Fe^0 particles in nickel chloride hexahydrate aqueous solution under mechanical stirring.

All solutions were prepared using deionized water and were deoxygenated in vacuum sealed bottles under N_2 atmosphere at ambient temperature. The Ni/Fe particles were washed with deionized water and stored in a vacuum oven. The structure and morphology of Ni/Fe particles were characterized by X-ray diffraction (XRD, X-ray 6000, Shimadzu, Japan) and field emission scanning electron microscopy (SEM, Sirion 200, FEI, USA). Energy dispersive X-ray (EDX) analysis was performed by EDX spectroscopy (Inca X-Max 50, Oxford instruments, UK) attached to field emission scanning electron microscope (FE-SEM, FEI Nova Nano SEM 450, Japan).

1.4. Dechlorination of 2,4-DCP solution by Ni/Fe nanoparticles

The batch experiments for dechlorination of 2,4-DCP were performed in 100 mL flasks sealed with rubber plugs containing 50 mL of 2,4-DCP solution and 0.5 g of Ni/Fe nanoparticles. The flasks were shaken at 120 r/min in a shaker at 25°C during the entire reaction time. The dechlorination efficiency of 2,4-DCP with different initial concentrations (13–50 mg/L) and pH values (3–7) was measured. pH was adjusted by adding dilute sulfuric acid solution or aqueous sodium hydroxide.

1.5. Analytical methods

At selected time intervals, the solid was separated from the solution by a 0.45 μm nylon membrane filter, and the residual 2,4-DCP concentration in solution was measured by a high-performance liquid chromatography system (SHIMADZU HPLC 2010-AT, Shimadzu, Japan). The mobile phase was methanol/water in the ratio of 60:40 (V/V), the flow rate was 1.0 mL/min, the injection volume was 20.0 μL, and the detector applied a ultraviolet light at 280 nm.

2. Results and discussion

2.1. Anodic process of iron in 2,4-DCP-containing aqueous solution

Anodic dissolution of iron is the driving force for the dechlorination of 2,4-DCP in the cathodic process. As an electron donor for dechlorination, the corrosion behavior of Fe should be carefully investigated.

2.1.1. Tafel polarization measurements of iron corrosion

Fig. 1 shows Tafel polarization curves recorded on the iron electrode in 0.1 mol/L Na_2SO_4 aqueous solution in the absence and presence of 2,4-DCP. With the addition of 2,4-DCP to the Na_2SO_4 solution, the value of corrosion current density I_{corr} increased significantly from 17.8 to 28.1 μA/cm^2, indicating that 2,4-DCP accelerated the corrosion rate of iron. The anodic Tafel curves showed that the anodic current density of the 2,4-DCP solution kept increasing when the potential increased, and the current density value was higher than that of the control solution (0 mg/L 2,4-DCP). The cathodic Tafel curves indicated that the hydrogen evolution reaction (HER) occurred on the iron electrode when the potential became more negative. H_2 from HER can absorb and dissociate on the iron electrode, and form atomic hydrogen radicals, reacting with 2,4-DCP. Thus, the catalytic hydrogenation reaction of 2,4-DCP could be enhanced, and more consumption of atomic hydrogen radicals may lead to the increase of cathodic current.

2.1.2. Effect of 2,4-DCP concentration on iron corrosion

The linear polarization curves and EIS were measured to study the effect of 2,4-DCP concentration on the anodic process. As shown in Fig. 2a, when the initial 2,4-DCP concentrations were 0, 20, 50, and 80 mg/L, the values of polarization resistance (R_p) were 716, 555, 516, and 434 Ω·cm^2, respectively. The result showed that R_p gradually decreased with the increase of the 2,4-DCP concentration.

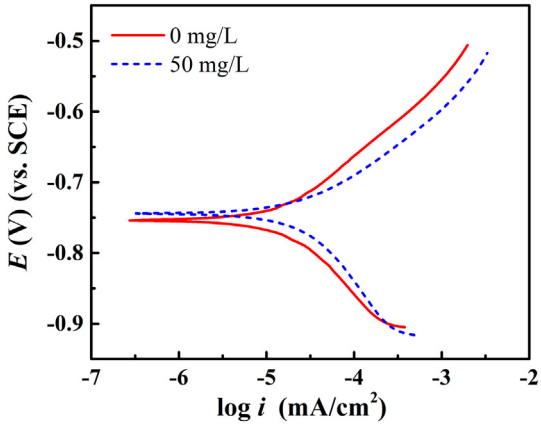

Fig. 1 – Tafel polarization curves for iron in 0.1 mol/L Na_2SO_4 aqueous solution in absence and presence of 2,4-dichlorophenol (2,4-DCP). E: potential; SCE: saturated calomel electrode; i: current density.

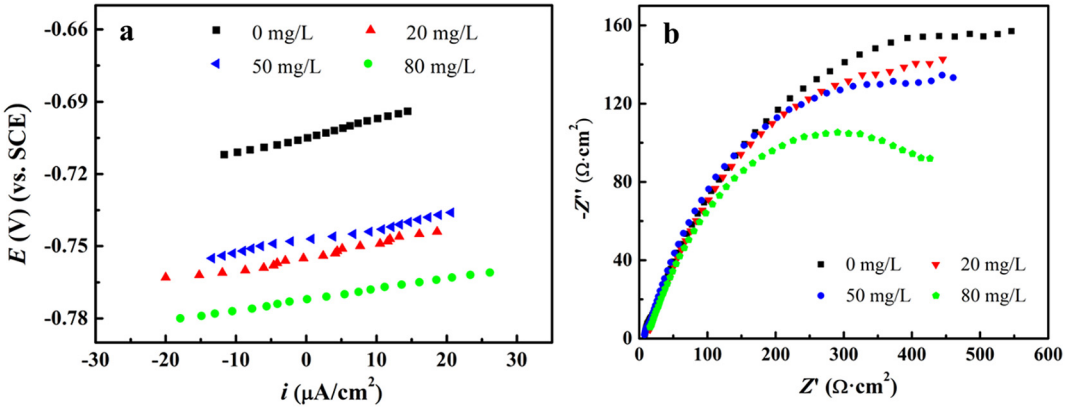

Fig. 2 – (a) Linear polarization curves and (b) Nyquist plots for iron in 0.1 mol/L Na_2SO_4 aqueous solution in presence of different concentration of 2,4-DCP at pH 7.0. Z′: the real part of the impedance; Z″: the imaginary part of the impedance.

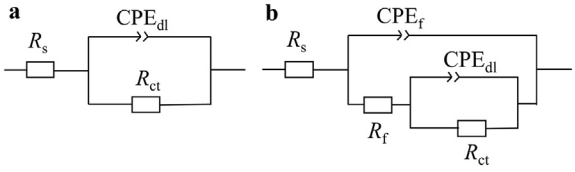

Fig. 3 – Equivalent circuits for the corrosion process of Fe in the (a) absence and (b) presence of 2,4-DCP. R_s: solution resistance; R_{ct}: charge transfer resistance; CPE_{dl}: constant phase element of the double layer; R_f: resistance of 2,4-DCP film at the iron surface; CPE_f: constant phase element of 2,4-DCP film at the iron surface.

The Nyquist plots for the Fe electrode in different concentration 2,4-DCP solutions are shown in Fig. 2b. Fig. 3 shows the electrochemical equivalent circuits to simulate the equivalent circuit, where R_s represents the solution resistance, CPE represents the constant phase element, R_{ct} represents charge transfer resistance, and R_f represents the resistance of 2,4-DCP film at the iron surface. The charge transfer resistances R_{ct} derived from Fig. 2b are listed in Table 1. When the initial concentrations of 2,4-DCP were 0, 20, 50, and 80 mg/L, the values of R_{ct} were 703, 473, 444, and 437 Ω·cm^2, respectively, indicating that the polarization resistances of iron corrosion decreased with the increase of 2,4-DCP concentration. The abovementioned two electrochemical measurements both indicated that the corrosion of iron was enhanced by adding 2,4-DCP. The acceleration effect could be promoted by increasing the initial concentration of 2,4-DCP in aqueous solution.

2.1.3. Effect of initial pH on iron corrosion

Fig. 4 shows the linear polarization curves and Nyquist plots of the anodic process in Na_2SO_4 aqueous solution in the absence and presence of 2,4-DCP at different pH. The values of R_p derived from the polarization curves in Fig. 4a are listed in Table 2. When the pH values were 3.0, 5.0, and 7.0, the values of R_p were 393, 452, and 516 Ω·cm^2, respectively. The results showed that R_p increased with the increase of pH. Fig. 4b shows that the diameters of semicircles for iron corrosion increased with the increase of initial pH from 3.0 to 7.0 in 2,4-DCP solution, indicating that charge transfer process at the interface showed an increasing trend (315, 376, and 444 Ω·cm^2, respectively). Therefore, the abovementioned two electrochemical measurements both indicated that the corrosion of iron was promoted by the decrease of pH ranging from 7.0 to 3.0.

2.2. Cathodic process on nickel surface in 2,4-DCP containing aqueous solution

2.2.1. Effect of 2,4-DCP concentration on cathodic process

To illustrate the electrochemical activity of the Ni electrode, LSV measurements of the Ni electrode in Na_2SO_4 aqueous solution containing different concentrations of 2,4-DCP were conducted. The result in Fig. 5 shows that an increase in cathodic current could be observed with an increase of the initial 2,4-DCP concentration from 0 to 125 mg/L. The reduction current densities on the Ni electrode at −0.75 V (vs. SCE) were 80, 106, and 111 μA/cm^2, for initial 2,4-DCP concentrations of 40, 80, and 125 mg/L.

For catalytic hydrogenation reduction, 2,4-DCP adsorbed on the surface of the Ni electrode, where C–Cl bonds could break. Then a hydrogen atom was able to replace the chlorine atom. The catalytic hydrogenation reaction can be approximately depicted by Eqs. (3)–(6).

During the cathodic process, hydrogen evolution and catalytic hydrogenation reduction of 2,4-DCP both took place. More 2,4-

Table 1 – Polarization resistance of iron in 0.1 mol/L Na_2SO_4 aqueous solution in presence of different concentrations of 2,4-DCP at pH 7.0.

Concentrations (mg/L)	0	20	50	80
LP R_p (Ω·cm^2)	716	555	516	434
EIS R_{ct} (Ω·cm^2)	703	473	444	437

LP: linear polarization; EIS: electrochemical impedance spectroscopy; R_P: polarization resistance.

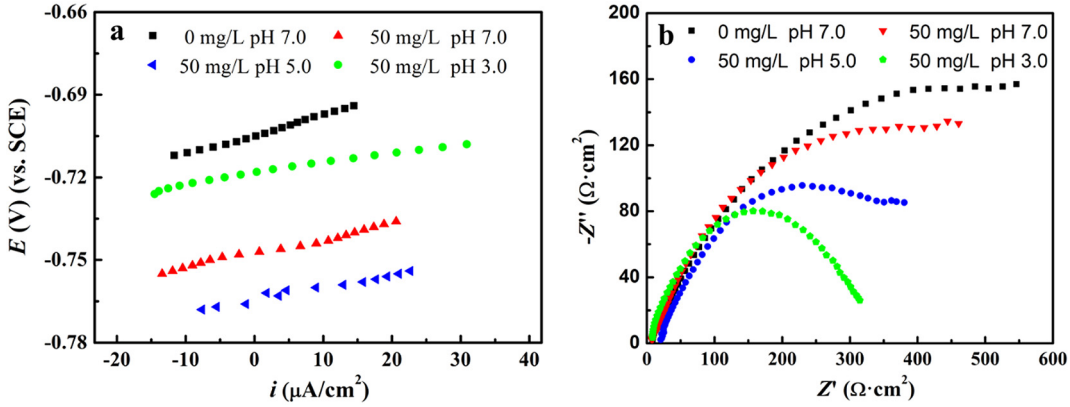

Fig. 4 – Linear polarization curves and (b) Nyquist plots for iron in 0.1 mol/L Na_2SO_4 aqueous solution in absence and presence of 2,4-DCP under different pH values.

Table 2 – Polarization resistance of iron in 0.1 mol/L Na_2SO_4 aqueous solution in absence and presence of 2,4-DCP under different pH values.

Concentrations (mg/L)	0	50	50	50
pH	7.0	7.0	5.0	3.0
LP R_p ($\Omega \cdot cm^2$)	716	516	452	393
EIS R_p ($\Omega \cdot cm^2$)	703	444	376	315

DCP took part in the dechlorination process on the Ni electrode with the increase of the initial concentration of 2,4-DCP. Therefore, the interfacial catalytic reaction was intensified and led to an increase in cathodic current. Catalytic hydrogenation on the nickel electrode reduced 2,4-DCP and consumed adsorbed hydrogen on the surface of the nickel electrode. Besides, the catalytic hydrogenation process may accelerate the hydrogen evolution process and enhance the hydrogen evolution current density in turn. Therefore, the process of 2,4-DCP catalytic hydrogenation reduction can be enhanced by increasing the concentration of 2,4-DCP.

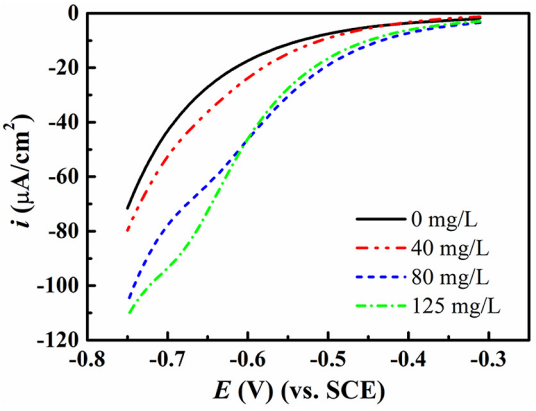

Fig. 5 – Linear scan voltammetry (LSV) curves of Ni electrode in Na_2SO_4 aqueous solution containing different concentrations of 2,4-DCP at pH 7.0.

2.2.2. Effect of initial pH on cathodic process

The electrocatalytic dechlorination was performed in Na_2SO_4 aqueous solution in the absence and presence of 2,4-DCP at different pH values. As illustrated in Fig. 6, the maximum reduction current density occurred at pH 5.0 in 2,4-DCP-containing solution, in contrast to other conditions. The reduction current density increased from pH 7.0 to 5.0. Atomic H adsorbed on the Ni surface at low pH values was beneficial for the reduction of 2,4-DCP. A higher concentration of H^+ can increase the amount of chemical adsorption of hydrogen on the surface of the nickel electrode, thus intensifying reaction between 2,4-DCP and adsorbed atomic H at the active sites of the Ni electrode surface. Intensified catalytic hydrogenation can consume more adsorbed hydrogen and accelerate the hydrogen evolution in return.

2.3. Dechlorination of 2,4-DCP by Ni/Fe nanoparticles

2.3.1. Characterization of Ni/Fe nanoparticles synthesized by chemical solution deposition

Ni/Fe nanoparticles with different Ni contents (5, 10, and 20 wt.%) were synthesized by chemical solution deposition. The morphology of the Ni/Fe particles was observed by SEM

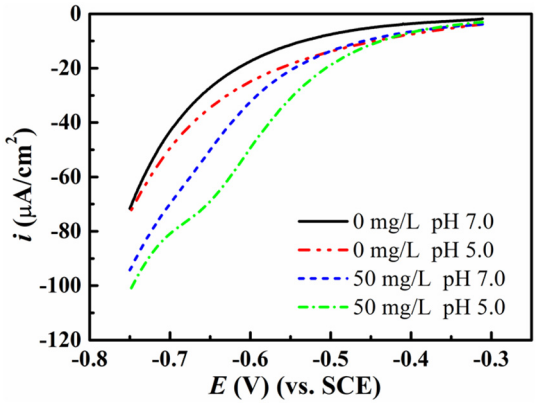

Fig. 6 – LSV curves of Ni electrode at pH 5.0 and 7.0.

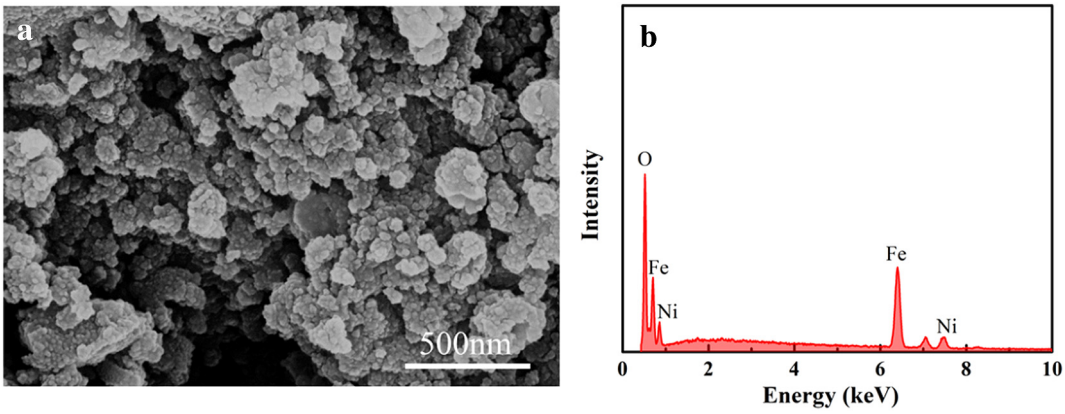

Fig. 7 – (a) Scanning electron microscopy (SEM) image and (b) energy dispersive X-ray (EDX) spectrum of Ni/Fe nanoparticles (Ni content: 20 wt.%).

(see Fig. 7a and Appendix A Fig. S1a and c). Most particles were less than 300 nm in size, indicating that the synthesized Ni/Fe particles were in the nanoscale range. The aggregation of a portion of the particles probably resulted from magnetic dipole interactions among the small metal particles (Zhu et al., 2011) and the reaction between Ni/Fe nanoparticles and H_2O in aqueous solution (Xu et al., 2009). EDX analysis results (see Fig. 7b and Appendix A Fig. S1b and d) showed the characteristic peaks of elements Fe, Ni, and O, confirming the partial oxidation of the Ni/Fe nanoparticles. The formation of an oxide layer on the core–shell particles surface probably occurred during preparation (Zhu et al., 2011). Notably, a corrosion coating on Fe^0 mainly consisting of Fe_3O_4 would form in water (Zhou et al., 2010).

2.3.2. Effect of 2,4-DCP concentrations on dechlorination by Ni/Fe bimetallic nanoparticles

Fig. 8 shows dechlorination results of 2,4-DCP by the prepared Ni/Fe nanoparticles with different initial 2,4-DCP concentrations (13, 32, and 50 mg/L) at pH 5.0. The final dechlorination efficiency of 2,4-DCP reached 52%, 66%, and 56%, respectively. Although the final dechlorination efficiencies of 2,4-DCP were similar, increase in the initial concentration of 2,4-DCP led to an increase of the total amount of dechlorinated 2,4-DCP. In the dechlorination reaction by Ni/Fe (or Pd/Fe) bimetallic nanoparticles, 2,4-DCP can be catalytically reduced to *o*-chlorophenol (*o*-CP) and *p*-chlorophenol (*p*-CP), and finally to phenol (Zhao et al., 2014; Zhang et al., 2010;). The Gibbs free energy (ΔG_f°) value of *o*-CP (−56.8 kJ/mol) is lower than that of *p*-CP (−53.1 kJ/mol), and thus, 2,4-DCP is more easily dechlorinated to *o*-CP (Xu et al., 2012b; Wang et al., 2013). Moreover, 2,4-DCP can also be reduced to phenol directly prior to the appearance of transitional products (Wei et al., 2006). The pathway for the catalytic dechlorination of 2,4-DCP is illustrated in Appendix A Fig. S2.

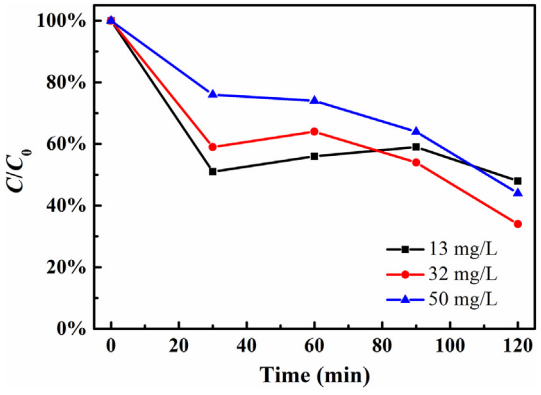

Fig. 8 – Effect of 2,4-DCP concentration on dechlorination efficiency with Ni/Fe nanoparticles. Reaction conditions: Ni/Fe dose 10 g/L, pH 5.0, and Ni content 20 wt.%. C: final 2,4-DCP concentration; C_0: initial 2,4-DCP concentration.

The formation of galvanic cells between the coupled Fe^0 and Ni led to continuous electron flow and catalytic activity enhancement. According to the results of the electrochemical experiments, the polarization resistance and charge transfer resistance decreased with the increase of initial concentration of 2,4-DCP, thus 2,4-DCP accelerated the corrosion process of iron. Simultaneously, the increase of 2,4-DCP concentration could provide more opportunity for 2,4-DCP to contact the active sites on the surface of catalytic nickel, where 2,4-DCP could obtain electrons and the hydrogenation dechlorination reaction was able to occur. Thus, the presence of more 2,4-DCP accelerated the catalytic hydrogen dechlorination process on the Ni surface. Therefore, both the anodic and cathodic electrode processes in the Ni/Fe bimetallic cell could be enhanced, so the increase of concentration (from 13 to 50 mg/L) was beneficial for dechlorination.

2.3.3. Effect of pH on dechlorination by Ni/Fe bimetallic nanoparticles

To investigate the pH effect on the dechlorination of 2,4-DCP, dechlorination experiments under different pH values ranging from 3.0 to 7.0 were analyzed. As shown in Fig. 9, the dechlorination efficiency of 2,4-DCP decreases with the increase of initial pH (from 3.0 to 7.0). From the abovementioned electrochemical experiment results, in the selected pH range, the polarization resistance and charge transfer resistance

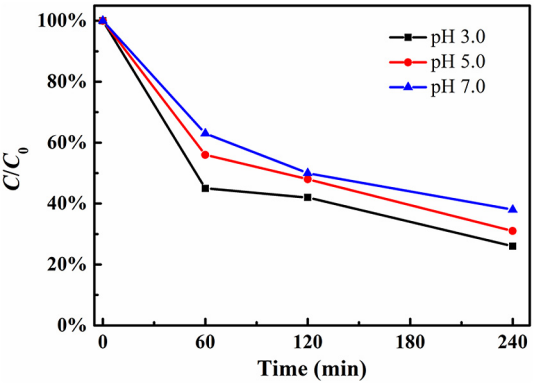

Fig. 9 – Effect of initial pH value on 2,4-DCP dechlorination efficiency with Ni/Fe nanoparticles. Reaction conditions: Ni/Fe dose 10 g/L, C_0 13 mg/L, and Ni content 20 wt.%.

showed a general decreasing trend with the increase of pH. The corrosion rate of iron was accelerated, and it became more likely to provide electrons for the reductive dechlorination of 2,4-DCP. The surface passivation layers composed of hydroxides or Fe_3O_4 on Fe/Ni nanoparticle surface were relatively difficult to form in more acidic solution. Therefore, the corrosion of iron and catalytic hydrogenation on the surface of nickel were not inhibited, leading to stable dechlorination activity during the reaction time, although the dechlorination of 2,4-DCP over Ni/Fe bimetal suffered from some limitation. However, some intermediates and products formed a passivation film at comparatively high pH values. The passivation film covering the particle surface blocked the reactive sites on the nanoparticle surface and retarded the dechlorination rate of 2,4-DCP.

According to Xu's study, at initial pH below 6.0, Ni/Fe could be used 10 times repeatedly (each time for 1 hr) for dechlorination and was still able to maintain comparatively high activity (Xu et al., 2012a). In addition, XRD and SEM-EDS mapping results of Ni/Fe nanoparticles before and after dechlorination and the results of six repeated dechlorination experiments in our work demonstrated that the Ni/Fe nanoparticles were relatively stable in dechlorination processes at pH 3.0 (Appendix A Figs. S3, S4, S5 and Section S1).

In addition, it was observed that cathodic process on the Ni electrode was enhanced at lower pH. This may be attributed to more significant transformation from adsorbed hydrogen to atomic hydrogen on the Ni surface, which was beneficial for the replacement of chlorine in the C–Cl bond. Furthermore, the influence of the Ni content of Ni/Fe nanoparticles was investigated at pH 3.0. Results showed that 10 wt.% Ni content was sufficient to obtain good dechlorination efficiency for 2,4-DCP (Appendix A Fig. S6).

3. Conclusions

The effects of pH and initial 2,4-DCP concentration on the dechlorination of 2,4-DCP by Ni/Fe bimetal and the corresponding electrode processes were systematically investigated. Electrochemical experiments suggested that 2,4-DCP had an acceleration effect on iron corrosion. The catalytic hydrogen reduction of 2,4-DCP on Ni was enhanced by the increase of 2,4-DCP concentration (≤125 mg/L). The decrease of the bulk pH facilitated both the catalytic hydrogenation and iron corrosion. The dechlorination experiments indicated that a relatively low pH was conducive to higher dechlorination efficiency of 2,4-DCP by Ni/Fe nanoparticles, which was consistent with the electrochemical measurements. At pH 3.0, the Ni/Fe nanoparticles could exist stably during the dechlorination processes, and 10 wt.% Ni loading into Ni/Fe bimetal was enough to achieve good dechlorination performance. Therefore, this study provides a better understanding of the reaction electrode processes of dechlorination of 2,4-DCP over Ni/Fe nanoparticles, which enables us to optimize the reaction conditions in practical application, i.e., the 2,4-DCP concentration and initial pH.

Acknowledgments

This work was supported by the National Natural Science Foundation of China (No. 51325102) and the Nature Science Foundation of Hubei Province of China (Team Project, No. 2015CFA017).

Appendix A. Supplementary data

Supplementary data to this article can be found online at https://doi.org/10.1016/j.jes.2019.01.012.

REFERENCES

Chen, X., Yao, X.Y., Yu, C.N., Su, X.M., Shen, C.F., Chen, C., et al., 2014. Hydrodechlorination of polychlorinated biphenyls in contaminated soil from an e-waste recycling area, using nanoscale zerovalent iron and Pd/Fe bimetallic nanoparticles. Environ. Sci. Pollut. Res. 21 (7), 5201–5210.

Crane, R.A., Scott, T.B., 2012. Nanoscale zero-valent iron: Future prospects for an emerging water treatment technology. J. Hazard. Mater. 211–212, 112–125.

Gupta, V.K., Ali, I., Saini, V.K., 2004. Removal of chlorophenols from wastewater using red mud: an aluminum industry waste. Environ. Sci. Technol. 38 (14), 4012–4018.

Jovanovic, G.N., Atwater, J.E., Žnidaršič-Plazl, P., Plazl, I., 2015. Dechlorination of polychlorinated phenols on bimetallic Pd/Fe catalyst in a magnetically stabilized fluidized bed. Chem. Eng. J. 274, 50–60.

Liu, Y., Yang, F., Yue, P.L., Chen, G., 2001. Catalytic dechlorination of chlorophenols in water by palladium/iron. Water Res. 35 (8), 1887–1890.

Pera-Titus, M., García-Molina, V., Baños, M.A., Giménez, J., Esplugas, S., 2004. Degradation of chlorophenols by means of advanced oxidation processes: a general review. Appl. Catal. B 47 (4), 219–256.

Phenrat, T., Saleh, N., Sirk, K., Tilton, R.D., Lowry, G.V., 2007. Aggregation and sedimentation of aqueous nanoscale zerovalent iron dispersions. Environ. Sci. Technol. 41 (1), 284–290.

Su, J., Lin, S., Chen, Z., Megharaj, M., Naidu, R., 2011. Dechlorination of p-chlorophenol from aqueous solution using bentonite

supported Fe/Pd nanoparticles: synthesis, characterization and kinetics. Desalination 280 (1), 167–173.
Wang, H., Wang, J.L., 2009. Comparative study on electrochemical degradation of 2,4-dichlorophenol by different Pd/C gas-diffusion cathodes. Appl. Catal. B 89 (1–2), 111–117.
Wang, X., Zhu, M., Liu, H., Ma, J., Li, F., 2013. Modification of Pd-Fe nanoparticles for catalytic dechlorination of 2,4-dichlorophenol. Sci. Total Environ. 449, 157–167.
Wang, X., Li, F., Yang, J., 2014. Polyvinyl pyrrolidone-modified Pd/Fe nanoparticles for enhanced dechlorination of 2,4-dichlorophenal. Desalin. Water Treat. 52 (40–42), 7925–7936.
Wang, X.Y., Le, L., Alvarez, P.J.J., Li, F., Liu, K.Q., 2015. Synthesis and characterization of green agents coated Pd/Fe bimetallic nanoparticles. J. Taiwan Inst. Chem. Eng. 50, 297–305.
Wei, J., Qian, Y., Liu, W., Wang, L., Ge, Y., Zhang, J., et al., 2014. Effects of particle composition and environmental parameters on catalytic hydrodechlorination of trichloroethylene by nanoscale bimetallic Ni-Fe. J. Environ. Sci. 26 (5), 1162–1170.
Wei, J., Xu, X., Liu, Y., Wang, D., 2006. Catalytic hydrodechlorination of 2,4-dichlorophenol over nanoscale Pd/Fe: Reaction pathway and some experimental parameters. Water Res 40 (2), 348–354.
Zhang, W.H., Xie, Q., Zhang, Z.Y., 2006. Catalytic reductive dechlorination of p-chlorophenol in water using Ni/Fe nanoscale particles. J. Environ. Sci. 19 (3), 362–366.
Xu, X.H., Wo, J.J., Zhang, J.H., Wu, Y.J., Liu, Y., 2009. Catalytic dechlorination of p-NCB in water by nanoscale Ni/Fe. Desalination 242 (1–3), 346–354.
Xu, F., Deng, S., Xu, J., Zhang, W., Wu, M., Wang, B., et al., 2012a. Highly active and stable Ni–Fe bimetal prepared by ball milling for catalytic hydrodechlorination of 4-chlorophenol. Environ. Sci. Technol. 46 (8), 4576–4582.
Xu, J., Lv, X., Li, J., Li, Y., Shen, L., Zhou, H., et al., 2012b. Simultaneous adsorption and dechlorination of 2,4-dichlorophenol by Pd/Fe nanoparticles with multi-walled carbon nanotube support. J. Hazard. Mater. 225, 36–45.
Xu, J., Tan, L., Baig, S.A., Wu, D., Lv, X., Xu, X., 2013. Dechlorination of 2,4-dichlorophenol by nanoscale magnetic Pd/Fe particles: Effects of pH, temperature, common dissolved ions and humic acid. Chem. Eng. J. 231 (17), 26–35.
Zahran, E.M., Bhattacharyya, D., Bachas, L.G., 2013. Reactivity of Pd/Fe bimetallic nanotubes in dechlorination of coplanar polychlorinated biphenyls. Chemosphere 91 (2), 165–171.
Zhang, W.H., Quan, X., Wang, J.X., Zhang, Z.Y., Chen, S., 2006. Rapid and complete dechlorination of PCP in aqueous solution using Ni-Fe nanoparticles under assistance of ultrasound. Chemosphere 65 (1), 58–64.
Zhang, Z., Shen, Q., Cissoko, N., Wo, J., Xu, X., 2010. Catalytic dechlorination of 2, 4-dichlorophenol by Pd/Fe bimetallic nanoparticles in the presence of humic acid. J. Hazard. Mater. 182 (1–3), 252–258.
Zhang, Q., Guo, Y., Huang, M., Li, H., Gu, C., 2015. Degradation of selected polychlorinated biphenyls by montmorillonite clay-templated Fe^0/Ni^0 bimetallic system. Chem. Eng. J. 276, 122–129.
Zhao, D.M., Zheng, Y.Y., Li, M., Baig, S.A., Wu, D.L., Xu, X.H., 2014. Catalytic dechlorination of 2,4-dichlorophenol by Ni/Fe nanoparticles prepared in the presence of ultrasonic irradiation. Ultrason. Sonochem. 21 (5), 1714–1721.
Zhou, T., Li, Y., Lim, T.-T., 2010. Catalytic hydrodechlorination of chlorophenols by Pd/Fe nanoparticles: Comparisons with other bimetallic systems, kinetics and mechanism. Sep. Purif. Technol. 76 (2), 206–214.
Zhou, H., Han, J., Baig, S.A., Xu, X., 2011. Dechlorination of 2,4-dichlorophenoxyacetic acid by sodium carboxymethyl cellulose-stabilized Pd/Fe nanoparticles. J. Hazard. Mater. 198 (2), 7–12.
Zhu, N.M., Zhang Li, Y., Zhang, F.S., 2011. Catalytic dechlorination of polychlorinated biphenyls in subcritical water by Ni/Fe nanoparticles. Chem. Eng. J. 171 (3), 919–925.